THE JOURNAL OF PHYSICAL CHEMISTRY LETTERS
A JOURNAL OF THE AMERICAN CHEMICAL SOCIETY

pubs.acs.org/JPCL
Letter

Effect of Covalence and Degree of Cation Order on the Luminous Efficacy of Mn^{4+} Luminescence in the Double Perovskites, Ba_2BTaO_6 (B = Y, Lu, Sc)

Alok M. Srivastava,* Mikhail G. Brik, Chong-Geng Ma, William W. Beers, William E. Cohen, and Michal Piasecki*

Cite This: J. Phys. Chem. Lett. 2024, 15, 4175−4184
Read Online

ABSTRACT: The spectroscopic properties of the Mn^{4+} ion are investigated in the series of isostructural double perovskite compounds, Ba_2BTaO_6 (B = Y, Lu, Sc). A comparison of these properties highlights the influence of covalent bonding within the perovskite framework and the degree of order between the B^{3+}−Ta cations on the energy and intensity of the $Mn^{4+2}E \rightarrow {}^4A_2$ emission transition (R-line). These two parameters of the emission spectrum are of importance for practical application since they determine the phosphor luminous efficacy. The influence of covalent bonding within the corner shared $BO_{6/2}$ and $TaO_{6/2}$ perovskite framework on the energy of the R-line energy is investigated. From the spectroscopic data, we have derived information on the influence of the degree of order between the B^{3+} and Ta^{5+} cations on the intensity of the R-line. The lowest energy and the highest intensity of the R-line are found in the double perovskite, Ba_2ScTaO_6. The purpose of this work is to propose for first time an explanation of these effects in the considered double perovskites. The obtained results are useful guidelines for practical improvement and tuning of key parameters of phosphors to the desired values.

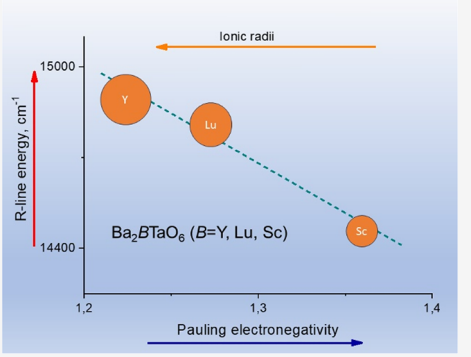

The modern-day phosphor converted light emitting diodes (pc-LEDs) are based on the blue emitting InGaN chip coated with a phosphor or a blend of phosphors that produces light of a specific spectral power distribution. The energy saving and cost-effective pc-LED technology has been developed for use in such diverse applications as displays, general illumination, traffic signals and horticultural lighting to name a few. The commercial success of the red emitting K_2SiF_6:Mn^{4+} (KSF/PFS) phosphor for general illumination application is traced to the sharp line emission spectrum that matches well with the human eye sensitivity curve. This provides for the construction of white light emitting diodes with high efficacy and good color rendering index.[1] The enormous market potential for such pc-LED devices has prompted the fundamental studies of the Mn^{4+} ion luminescence in diverse compounds such as fluoride, oxides, and oxyfluoride.[1−5] These ongoing fundamental inquiries are taking place at a very rapid pace.

The luminescence of the Mn^{4+} ion, with the $3d^3$ electronic configuration, is composed of the ${}^2E \rightarrow {}^4A_2$ sharp line transition (R-line; zero-phonon line or ZPL) accompanied by the Stokes and anti-Stoles vibronic sidebands. The emission spectrum of the Mn^{4+} ion can be tuned to satisfy the requirement of a particular pc-LED device. For general illumination application, the phosphor must generate high luminous efficacy (lumens per watt or LPW). High LPW is attained when the emission spectrum makes a good match with the human eye response function (luminosity response function). Our fundamental studies have established two factors of importance for high LPW, (1) the energy (emission wavelength) and (2) the intensity of the Mn^{4+} spin-forbidden ${}^2E \rightarrow {}^4A_2$ emission transition.[1,6] The phosphor luminous efficacy is maximized in host crystals which support high energy and high intensity of the R-line. Therefore, it is instructive to inquire about the properties of the host lattice that maximize the luminous efficacy.

In the Tanabe-Sugano diagram for the ions with d^3 electron configuration, the energy of the ${}^2E$ state is independent of the crystal field strength (Dq). The energy of the ${}^2E \rightarrow {}^4A_2$ emission transition is determined chiefly by the covalence of the "Mn^{4+}−ligand" bonding.[7−9] A blue or a red shift of the emission spectrum can be induced by altering the bonding covalence. In highly ionic compounds such as fluorides, the

Received: January 20, 2024
Revised: April 3, 2024
Accepted: April 5, 2024
Published: April 10, 2024

https://doi.org/10.1021/acs.jpclett.4c00205
J. Phys. Chem. Lett. 2024, 15, 4175−4184

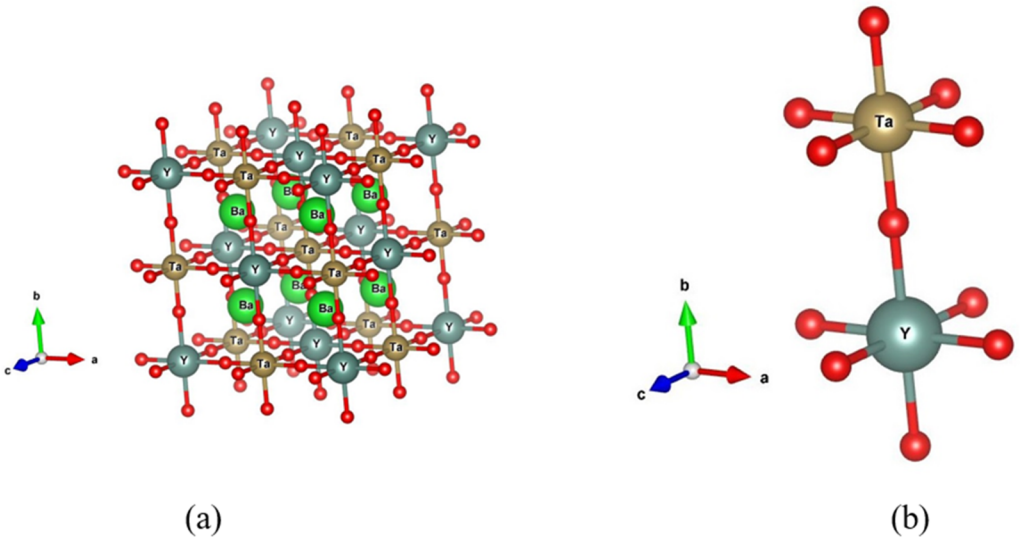

Figure 1. (a) The unit cell of Ba_2YTaO_6 and (b) the linear [Y−O−Ta] linkage. Drawn by VESTA.[17]

Table 1. Crystallographic Data of Cubic (Space Group $Fm\bar{3}m$) Double Perovskites $BaBTaO_6$ (B = Y, Lu, Sc)[a]

	Lattice constant (Å)	Unit cell volume (Å^3)	*B*-0 (Å)	*Ta*-0 (Å)	$R_{B^{3+}}$ (Å)	*t*
Ba_2YTaO_6	8.43539	600.23	2.232	1.986	0.90	0.98
Ba_2LuTaO_6	8.3760	587.64	2.203	1.985	0.861	0.99
Ba_2ScTaO_6	8.226	556.5	2.0894	2.0236	0.745	1.02

[a]*B-0* and *Ta*-0 are the bond distances (Å). $R_{B^{3+}}$ is Shannon's ionic radii of six coordinated *B* cations.[20] The data for Ba_2ScTaO_6 are from ref 20. The data for *B* = Y, Lu are from ICSD. *t* is the tolerance factor calculated using eq 1.

emission is blue-shifted relative to oxidic compounds with higher covalent character.

The intensity of the R-line is determined by the site symmetry: the higher the point symmetry of the impurity ion site, the lower is the R-line intensity, and vice versa.[6] The presence or absence of an inversion center at the Mn^{4+} ion site is key to the strength of the R-line. In a site with inversion symmetry, the parity selection rule cannot be lifted by the odd-parity crystal field components. In such sites, the R-line has magnetic dipole character with low oscillator strength. In this case, the R-line has weak intensity relative to the vibronic sidebands which have a much larger oscillator strength since they are electric-dipole allowed transitions. In sites lacking inversion symmetry, the R-line gains intensity relative to the vibronic sidebands due to the relaxation of the parity selection rule. Increase in R-line intensity has important practical consequences since it causes color changes which increase the phosphor luminous efficacy.[1,6]

In a site where the Mn^{4+} ion has near or ideal octahedral symmetry with respect to the nearest neighbor anions, it is possible to increase the R-line intensity by deliberately creating cationic disorder in the second coordination sphere (next-nearest neighbor cations). We explored this approach to increasing R-line intensity with solid solution systems that provided random cation distribution in compounds crystallizing with the pyrochlore[10] and double perovskite structures.[11] The site disorder in the second coordination sphere increased the R-line intensity by lowering the symmetry around the Mn^{4+} ion. Different cations in the second coordination sphere with different ionic radii and electronegativities can alter Mn^{4+}−ligand bond distances and ligands' effective charges. These changes in the geometric and electronic parameters can remove the inversion center in the impurity cluster. More recently, we reported on the influence of deliberately induced cationic disorder on the optical properties of Cr^{3+} in spinel oxides.[12]

It is of fundamental and practical interest to inquire about the structural and chemical bonding factors which influence the energy and intensity of the $Mn^{4+2}E \rightarrow {}^4A_2$ emission transition. Our approach to this inquiry is to investigate the influence of compositional variations on the spectroscopic properties of the Mn^{4+} ion in a series of isostructural compounds. In the spirit of this approach, we have reported on the luminescence of Mn^{4+} ion in double perovskite compounds with varying compositions.[5,11,13−15] Such studies unravel composition−optical properties relationships. In this work, we report on a comparative study of the spectroscopic properties of the Mn^{4+} ion in a series of double perovskite compounds with the general formula Ba_2BTaO_6 (B = Y, Lu, Sc). The study highlights the influence of bonding covalence and degree of *B*−Ta cation mixing on the luminescence of the Mn^{4+} ion.

The synthesized material in powder form was examined by X-ray diffraction to determine the crystal structure and lattice site occupation. The double perovskite $A_2BB'O_6$ is derived from the simple perovskite, ABO_3, by ordering of *B* and *B*′ cations in alternate octahedral sites. The Ba_2BTaO_6 (B = Y, Lu, Sc) compounds crystallize in the cubic structure with space group $Fm\bar{3}m$. In Figure 1 are shown the unit cell of Ba_2YTaO_6 and the characteristic linear [−Y−O−Ta−] linkage. In the fully ordered arrangement, each Y cation has only Ta as the next nearest neighbor and vice versa. However, this ordering is never complete, and some degree of mixing between the *B* and Ta cations occurs. The degree of order is determined by the difference between the ionic size and charge of the *B* and Ta

https://doi.org/10.1021/acs.jpclett.4c00205
J. Phys. Chem. Lett. 2024, 15, 4175−4184

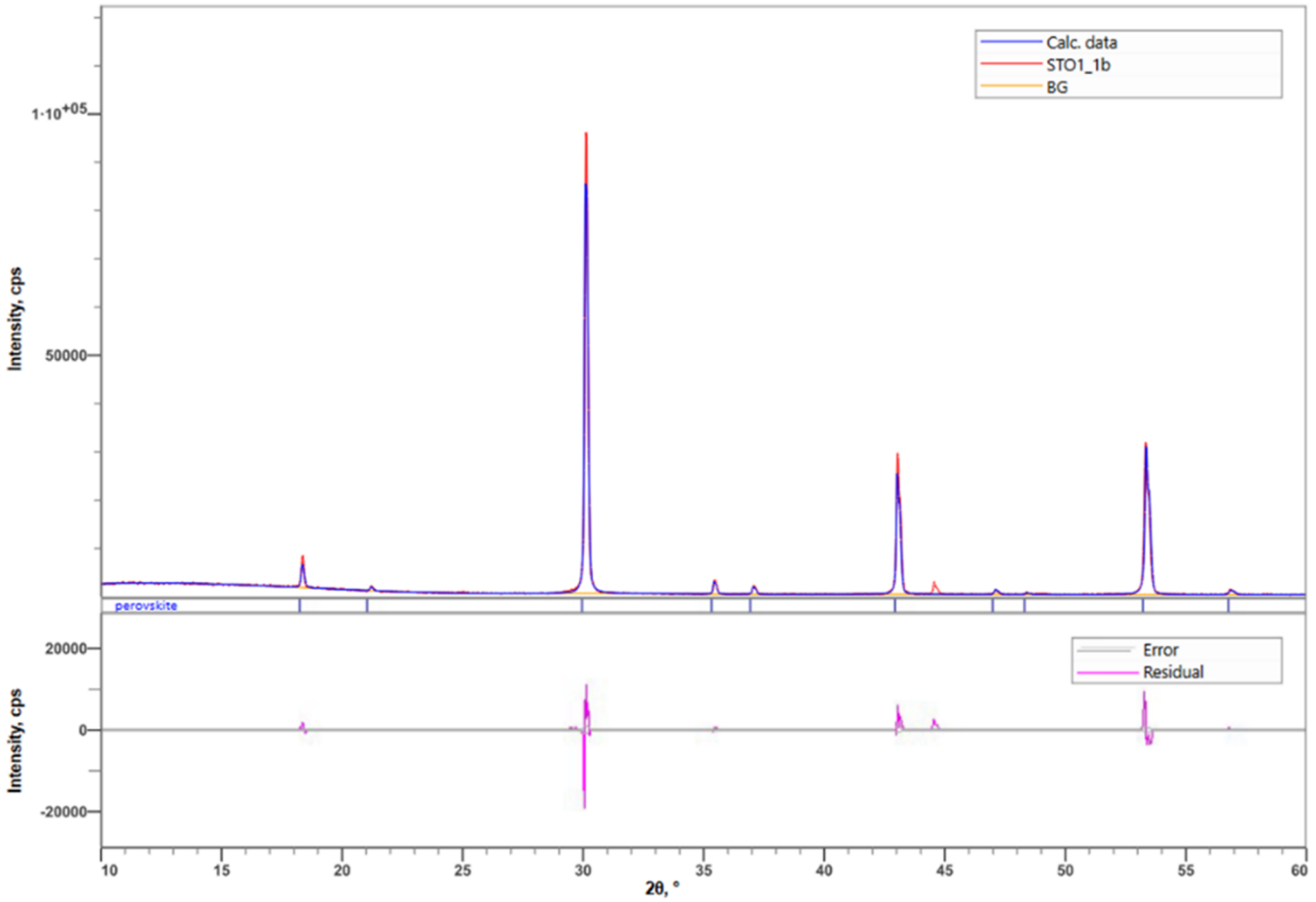

Figure 2. X-ray diffraction powder pattern of cubic $Ba_2Y(Ta_{0.99}Mn_{0.01})O_6$. The sample was found to be phase-pure.

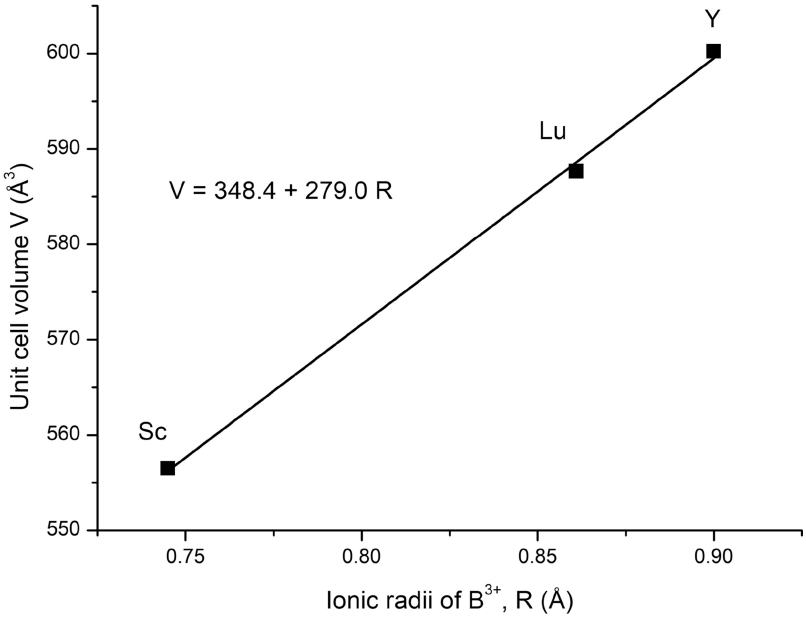

Figure 3. Unit cell volume plotted against the ionic radii of B^{3+} cation for Ba_2BTaO_6 (B = Y, Lu, Sc).

cations.[16] It is also determined by the process employed in the synthesis of these compounds.

The Goldschmidt geometric tolerance factor t for the double perovskite with the general formula $A_2BB'O_6$ can be written as[16]

$$t = \left[\frac{r_A + r_0}{\sqrt{2}\left(\frac{r_B + r_{B'}}{2} + r_0\right)}\right] \quad (1)$$

https://doi.org/10.1021/acs.jpclett.4c00205
J. Phys. Chem. Lett. 2024, 15, 4175−4184

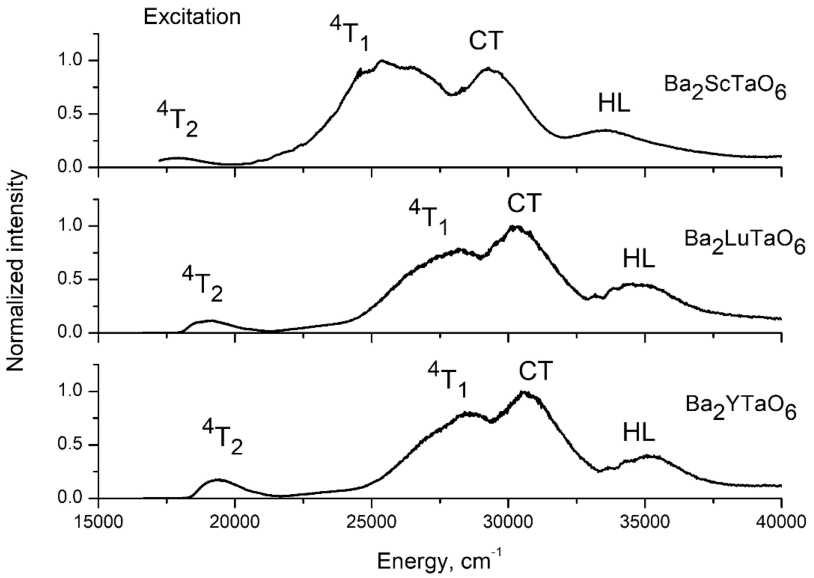

Figure 4. Excitation spectra for Mn^{4+} luminescence of Ba_2YTaO_6 (λ_{em}= 685 nm), Ba_2LuTaO_6 (λ_{em}= 689 nm), and Ba_2ScTaO_6 (λ_{em}= 708 nm) at T = 12 K.

Table 2. Energies of the Mn^{4+} Transitions in the Excitation Spectra of $BaBTaO_6$ (B = Y, Lu, Sc) at T = 12 K[a]

	HL	CT	$^4A_2 \rightarrow {}^4T_1$	$^4A_2 \rightarrow {}^4T_2$	Dq	Ref
Ba_2YTaO_6	34 842	30 581	28 570	19 230	1923 (1879)	This work
Ba_2YTaO_6	35 000	30 810	27 745	18 950	1895	21
Ba_2LuTaO_6	34 129	30 248	28 012	18 996	1899 (1832)	This work
Ba_2LuTaO_6	34 129	30 303	27 397	18 518	1852	22
Ba_2ScTaO_6	33 333	29 154	25 303	17 857	1785 (1715)	This work

[a]HL is host lattice absorption; CT is the $O^{2-} \rightarrow Mn^{4+}$ charge transfer transition. The room temperature Dq values are in parentheses. The literature data for Ba_2YTaO_6[21] and Ba_2LuTaO_6[22] are at room temperature. All values in cm^{-1}.

where r_A is the ionic radii of the A cation in 12-fold coordination, r_B and $r_{B'}$ are the ionic radii of B and B' ions in 6-fold coordination, and r_0 is the ionic radii of the oxygen ion (1.40 Å). The value of t reflects the stability of the perovskite structure. The highest stability occurs for t = 1, which corresponds with the ideal perovskite structure. The tolerance factor for Ba_2BTaO_6 compounds, listed in Table 1, is close to 1. This is consistent with their cubic symmetry as determined by X-ray diffraction. It implies that the B−O−Ta bonds are 180° (linear) and the $BO_{6/2}$ and $TaO_{6/2}$ units are perfect octahedrons.

The double perovskite compounds were found to be single phase materials by their X-ray diffraction patterns. As an example, we exhibit the X-ray diffraction pattern of the $Ba_2Y(Ta_{0.99}Mn_{0.01})O_6$ compound in Figure 2.

The crystallographic data for the double perovskites that are relevant to our discussion are assembled in Table 1. We have indicated in the Introduction that a goal of this work is to inquire about the influence of the degree of order between B−Ta cations on the Mn^{4+} luminescence. This ordering is never complete and is driven by the differences between the charges and ionic radii of the cations.[16] Cationic disorder can affect the unit cell volume of the double perovskite compound. For example, if Ta^{5+} replaces a B-cation in the [B−O−Ta] linkage of Ba_2BTaO_6, then it will have another highly charged Ta^{5+} as its next neighbor cation (see Figure 1). The resulting electrostatic repulsion due to this antisite disorder will increase the lattice constant or the unit cell volume. To check for any evidence of B−Ta antisite disorder within the available crystallographic data, the unit cell volume of Ba_2BTaO_6 (B = Y, Lu, Sc) as a function of the B-cation ionic radii was plotted (Figure 3). The ionic radii are tabulated by Shannon.[18] We can see that the cell volume increases linearly as ionic radii of the B-cation increase. Therefore, any B−Ta antisite disorder is not seen in the lattice constant data that are obtained by X-ray diffraction. As we will show in the later sections, the luminescence data are more sensitive techniques for probing order−disorder phenomena.

The interpretation of the optical data requires the knowledge of the host lattice site substituted by Mn^{4+}. In these double perovskite compounds, there are two octahedral sites available for substitution. Note from the Experimental Section that the compositions are formulated as $Ba_2B(Ta_{0.99}Mn_{0.01})O_6$. Nonetheless, it may be argued that in the synthesized sample, the substitution $2Mn^{4+} \rightarrow B^{3+} + Ta^{5+}$ is favored since it ensures charge balance.

However, ionic radii consideration reasons against such substitution. The ion size difference between Mn^{4+} (0.54 Å) and Sc^{3+} (0.745 Å), which is the smallest B cation in this series of compounds, is ∼40%. In contrast, the ion size mismatch between Mn^{4+} and Ta^{5+} is ∼20%. To minimize local elastic strain effects or lattice distortions, the impurity Mn^{4+} ion will preferentially substitute at the octahedral Ta^{5+} site in Ba_2BTaO_6 (B = Y, Lu, Sc). This reasoning is supported by computational modeling of the site occupation and defect formation in the isostructural niobate, Ba_2YNbO_6:Mn^{4+}. The result shows that the occupation of the Nb^{5+} site is preferred

https://doi.org/10.1021/acs.jpclett.4c00205
J. Phys. Chem. Lett. 2024, 15, 4175−4184

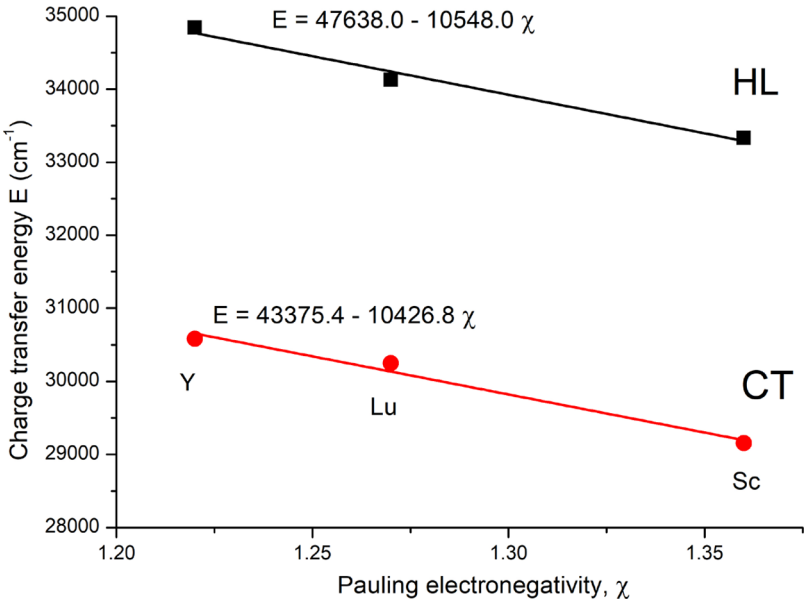

Figure 5. Relationship between the energies of the host lattice absorption (HL; $O^{2-} \rightarrow Ta^{5+}$ charge transfer) and the $O^{2-} \rightarrow Mn^{4+}$ charge transfer transition (CT) and the electronegativity of the *B*-cation (on the Pauling scale) in Ba_2BTaO_6 (*B* = Y, Lu, Sc).

with the charge compensation taking place via an antisite disorder (using the Kröger-Vink notation):[19]

$$2MnO_2 + 2Nb_{Nb} + Y_Y 2Mn'_{Nb} + Nb^{\cdot\cdot}_Y + 0.5Y_2O_3 + 0.5Nb_2O_5$$

The low temperature (T = 12 K) excitation spectra of Ba_2BTaO_6:Mn^{4+} (B = Y, Lu, Sc,) are shown in Figure 4. The excitation spectra consist of four major bands corresponding with the host lattice absorption (HL), the $O^{2-} \rightarrow Mn^{4+}$ charge transfer transition (CT), and the spin-allowed but parity-forbidden (as taking place between the states of the $3d^3$ electron configuration without changing the states' parity) $^4A_2 \rightarrow {}^4T_1$ and $^4A_2 \rightarrow {}^4T_2$ transitions. In Table 2 are assembled the transition energies along with the room temperature data that are available on two of these double perovskite compounds in archival literature.

We first discuss the compositional dependence of the host lattice absorption energy (HL). The absorption is due to the $O^{2-} \rightarrow Ta^{5+}$ charge transfer transition which involves the transfer of an O-2p electron to the empty t_{2g} (π-bonding) orbital of the Ta^{5+} ion. It increases in the order, Sc < Lu < Y and is, therefore, correlated with the *B*-cation. Band gap energies of Ba_2ScTaO_6 and Ba_2YTaO_6, which are obtained from band-structure calculations, are 3.35 eV (27 019 cm^{-1}) and 3.99 eV (32 181 cm^{-1}), respectively.[23] The observed trend can be rationalized from the results of electronic structure calculations of the compounds, which establish the degree of covalency (hybridization) between the orbitals of *B*−Ta cations and oxygen 2p orbitals. It should be noted that due to the ordering of *B* and Ta cations, each oxygen ion will have Ta^{5+} with the $5d^0$ electronic configuration on one side and the *B*-cation on the other side (Figure 1). In an octahedral coordination, the crystal field splits the 5-fold degenerate (in the free ion) d levels into lower 3-fold-degenerate t_{2g} (d_{xy},d_{yz},d_{xz}) and the upper 2-fold-degenerate e_g (d_{z^2},$d_{x^2-y^2}$) levels. The Ta−O bonding involves the hybridization between the O $2p_\pi$ and the Ta t_{2g} orbitals.

The band-structure of Ba_2ScTaO_6 has been reported.[20] The Sc^{3+} ion, with the $3d^0$ electronic configuration, has empty d orbitals for covalent bonding with the O $2p_\pi$ orbitals. Therefore, in the [$ScTaO_6$] framework of Ba_2ScTaO_6, the π bonding between O $2p_\pi$ orbitals and Sc/Ta t_{2g} orbitals occurs on both side of each oxygen ion. This bonding character is reflected in the calculated band-structure. The conduction band is a mixture of Sc 3d and strongly hybridized Ta−O antibonding states. The conduction band edge is composed of the Ta 5d orbitals because the Ta−O hybridization is stronger than the Sc−O hybridization. This is because of the following factors: (1) the higher electronegativity of Ta (1.5 on the Pauling scale) relative to Sc (1.36), (2) the larger radial extension of the 5d orbital than the 3d orbital, and (3) the smaller Ta−O bond distance. The consequence of stronger Ta−O hybridization is the larger crystal field splitting (the t_{2g}−e_g separation) of the Ta 5d state (~5.5 eV) than that of the Sc 3d state (~2.2 eV). For this reason, the edge of the conduction band is composed of the Ta 5d orbitals.

The band-structure of Ba_2YTaO_6 shows a relatively smaller energetic overlap between the Y 4d and the O 2p states.[23] The calculated band-structure of the Lu-phase is like that of the Y-phase.[24] In these compounds, the π bonding with the Ta t_{2g} orbital occurs only on one side of each oxygen ion. The structural and electronic isolation of the TaO_6 octahedron appreciably narrows the conduction band and increases the band gap of Ba_2YTaO_6 relative to Ba_2ScTaO_6. We digress briefly to point out that the narrowing of the conduction band in compounds with the double perovskite structure has a profound influence on the optical properties of impurity ions. The conduction band narrowing that resulted from the isolation of the TiO_6 octahedral group and the deviation of the Mg−O−Ti bond angle from the ideal 180° in the double perovskite La_2MgTiO_6 was responsible for first observation of the localized $Bi^{3+3}P_{0,1} \rightarrow {}^1S_0$ emission in a titanate host.[25,26]

As suggested in ref 23, the band gap of these double perovskite compounds is an accurate indicator of the $O^{2-} \rightarrow Ta^{5+}$ charge transfer energy (HL). Figure 5 shows that HL decreases almost linearly as the electronegativity of the *B*-

https://doi.org/10.1021/acs.jpclett.4c00205
J. Phys. Chem. Lett. 2024, 15, 4175−4184

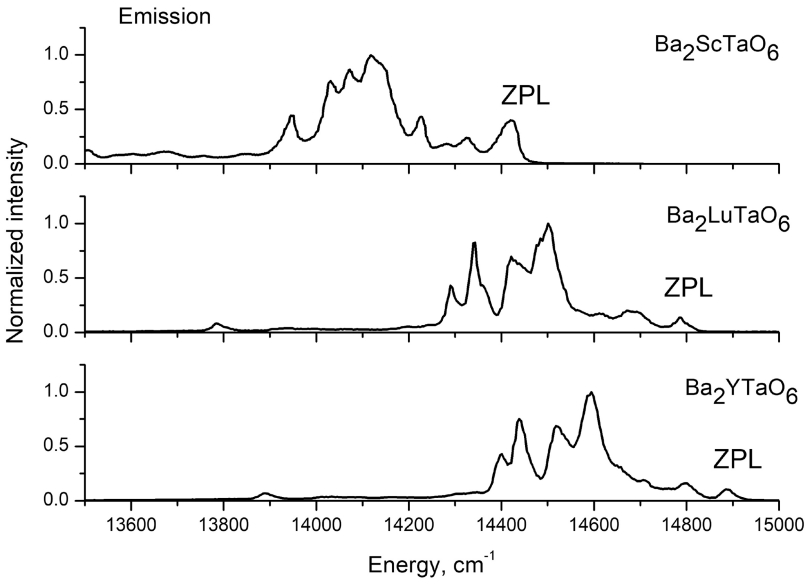

Figure 6. Emission spectra for Mn^{4+} luminescence of Ba_2YTaO_6 (λ_{ex}= 330 nm), Ba_2LuTaO_6 (λ_{ex}= 330 nm), and Ba_2ScTaO_6 (λ_{ex}= 390 nm) at T = 12 K. The R-line (ZPL) is identified in the spectra.

cation increases (on the Pauling scale). This leads to the conclusion that the covalent bonding within the perovskite framework of Ba_2BTaO_6 increases in the sequence, Y< Lu < Sc. That the scandate perovskite is most covalent is not surprising since the Sc^{3+} ion, with the $3d^0$ electronic configuration, has empty d-orbitals for covalent bonding with the oxygen anion, as discussed previously.

The compositional dependence of the CT is also associated with the *B*-cation electronegativity (Figure 5). Furthermore, both the HL and the CT decrease at the same linear rate with respect to electronegativity and framework covalency. Thus, the energy difference between the O 2p and the Mn^{4+} 3d orbitals decreases as the covalence of perovskite framework increases in the Ba_2BTaO_6 compounds.

The energy difference between the $^4A_2$ ground and $^4T_2$ excited states is the strength of the octahedral crystal field, Δ_o = 10 *Dq*. The values of *Dq* are calculated by the formula, $E(^4A_2 \rightarrow {}^4T_2)/10 = Dq$, where $E(^4A_2 \rightarrow {}^4T_2)$ is the peak energy of the optical transition. The point charge model of crystal field predicts *Dq* to vary as R^{-5}, where R is the "Mn^{4+}–ligand" bond distance. In real systems, the power of R can be considerably different due to factors such as covalence which is neglected in the point charge model.[27] The experimental *Dq* parameters can be analyzed in terms of the Ta–O bond distances. Since the local relaxation around the impurity ion will be different in the three perovskite compounds, the relaxed Mn–O bond distances R(Mn–O)) were calculated from the Ta–O bond distances (R(Ta–O)) and the ionic radii of Mn^{4+} ($r_{Mn^{4+}}$), Ta^{5+} ($r_{Ta^{5+}}$), and oxide ($r_{o^{2-}}$) ions by the formula:

$$R(Mn{-}O) = R(Ta{-}O)\frac{r_{Mn^{4+}} + r_{O^{2-}}}{r_{Ta^{5+}} + r_{O^{2-}}} \quad (2)$$

The relaxed R(Mn–O) bond distances are 1.878 Å for the Y/Lu-phases and 1.976 Å for the Sc-phase. The lower *Dq* = 1785 cm^{-1} for the scandate perovskite is consistent with the longer R(Mn–O) relative to the Y (*Dq* = 1923 cm^{-1}; 1.878 Å) and Lu (*Dq* = 1899 cm^{-1}; 1.878 Å)-phases. Note that despite the same R(Mn–O), *Dq* is slightly smaller in Ba_2LuTaO_6 than that in Ba_2YTaO_6. This shows the effect of the next nearest neighbor cations on *Dq*. In the [–*B*–O–Mn–] linkage, the Lu^{3+} with the smaller ionic radii will bond more strongly with the oxide ion than the larger Y^{3+} ion. The formal charge on the O^{2-} is expected to be smaller for *B* = Lu, which decreases *Dq*. Also given in Table 2 are values of *Dq* at room temperature. The increase in the strength of the crystal field at low temperature is due to shortening of the Mn–O bond by thermal contraction.

The pattern in the excitation spectra is different between the scandate and Y/Lu-phases. The $O^{2-} \rightarrow Mn^{4+}$ charge transfer transition (CT) is the most intense band in the excitation spectra of Y and Lu-perovskites (see Figure 4). In Ba_2ScTaO_6, the $^4A_2 \rightarrow {}^4T_1$ transition is relatively stronger. The lowest energy of the $O^{2-} \rightarrow Mn^{4+}$ transition is found in this perovskite (Table 2). An increase in nonradiative energy loss with decreasing ligand-to-metal charge transfer energy is not uncommon.[28] Therefore, the radiative efficiency under $O^{2-} \rightarrow Mn^{4+}$ charge transfer excitation is lower since it provides for a more efficient nonradiative pathway for the excitation energy to decay directly to the ground state in the scandate perovskite.

The low temperature (T = 12 K) emission spectra of Ba_2BTaO_6:Mn^{4+} (*B* = Y, Lu, Sc,) are exhibited in Figure 6. At this temperature, the emission spectra are composed of the R-line and their associated Stokes vibronic bands, which correspond with the ungerade modes of the [MnO_6] octahedral moiety.[3] The energies of these lines are summarized in Table 3. The energy of the vibronic sidebands matches well with the data reported for [MnO_6] moiety in the double perovskite, Ba_2GdNbO_6.[29]

The influence of covalency on the emitting ^2E energy level is clearly seen in the emission spectra. In the Tanabe-Sugano diagram for the d^3 configuration, the energy of $^2E \rightarrow {}^4A_2$ emission transition depends on the covalence of the Mn–O bonding.[7−9] The data assembled in Table 3 indicate the following order of Mn–O bond covalency in Ba_2BTaO_6, Y< Lu < Sc. Generally, a specific parameter that influences the R-line energy in perovskite oxides is the deviation of the O–Mn–O bond angle from ideal octahedral 90°.[30,31] The angular deviation decreases the hybridization between Mn^{4+} t_{2g} ($d\pi$) and O $2p_\pi$ orbitals. The reduced Mn–O bond covalence raises

https://doi.org/10.1021/acs.jpclett.4c00205
J. Phys. Chem. Lett. 2024, 15, 4175−4184

Table 3. Energy of the R-Line and the Stokes Vibronic Lines in the Emission Spectra of Ba_2BTaO_6:Mn^{4+} (B = Y, Sc, Lu) at T = 12 K[a]

	R-line (ZPL)	Lattice modes	ν_6 (t_{2u}; bend)	ν_4 (t_{1u}; bend)	ν_3 (t_{1u}; stretch)
Ba_2YTaO_6	14 885	88/179/227	291	367	447/485
Ba_2LuTaO_6	14 788	104/177	287	366	450/499
Ba_2ScTaO_6	14 415	95/137/193	297	342/384	470
Ba_2GdNbO_6	15 059	-	280	364	434/449

[a]All values in cm^{-1}. The data for Ba_2GdNbO_6 are from ref 29.

the R-line energy. In cubic Ba_2BTaO_6 (B = Y, Lu, Sc), the Ta−O−Ta bond angles are perfect 90°.Therefore, the R-line energy is determined by the covalence of the perovskite framework, which increases in the same sequence, Y< Lu < Sc. As shown in Figure 7, the energy of the R-line decreases linearly with increasing electronegativity of the B-cation in Ba_2BTaO_6 (B = Y, Lu, Sc). The Mn^{4+} ion is most covalently bonded in the Sc-phase and least in the Y-phase.

It is pointed out that while the R-line and the vibronic sidebands have sharp features in Ba_2BTaO_6 (B = Y, Lu), they are broadened in the Sc-phase. It is also pointed out that the R-line is considerably more intense in the Sc-phase than in the other two phases. These properties are accounted for in the next section.

In Table 4 are assembled the values of the Racah parameters B, C (along with the crystal field strength Dq) for the Mn^{4+} ion. The parameters were estimated from the excitation and emission spectra of the considered double perovskites with the help of standard equations for the energy levels of the d^3 electron configuration.[32] In addition, the values of the new nephelauxetic parameter $\beta_1 = \sqrt{\left(\frac{B}{B_0}\right)^2 + \left(\frac{C}{C_0}\right)^2}$ [9] were calculated; B_0 = 1160 cm^{-1}, C_0= 4303 cm^{-1} are the Racah parameters for the free Mn^{4+} ion.[33]

The β_1 parameter reflects the reduction of the Racah parameters caused by covalent bonding when the ion is

Table 4. Spectroscopic Parameters for the Mn^{4+} Ions (All in cm^{-1}) in $BaBTaO_6$ (B = Y, Lu, Sc) Double Perovskites

	B	C	Dq	β_1	Ref
Ba_2YTaO_6	1019	2560	1923	1.061	This work
Ba_2LuTaO_6	971	2627	1899	1.036	This work
Ba_2ScTaO_6	756	2958	1785	0.947	This work

embedded in a host compound.[9] The smaller the value of β_1, the higher is the covalence of the Mn−O bonding. The data indicate that the Mn−O bonding covalency increases in the sequence, Y < Lu < Sc. This is exactly as derived from the structural peculiarities of these double perovskite frameworks and influence of the second cation on the Mn^{4+} spectroscopic properties.

In the next step, we show that the intensity of the Mn^{4+} R-line is correlated with the degree of order between the B−Ta cations in Ba_2BTaO_6. In Table 5 are listed the peak intensity ratios of the R-line to its most intense Stokes ν_6 sideband (R_I). Also listed are the ionic radii differences between the B−Ta cations. The Shannon ionic radius of 6-fold coordinated Ta^{5+} ion is 0.64 Å.[18] Clearly, R_I depends on the ionic radii difference between the B−Ta cations. It increases considerably in the Sc-phase.

Table 5. Peak Intensity Ratio of the Mn^{4+} R-Line (ZPL) to the Most Intense Vibronic Sideband (ν_6) in $BaBTaO_6$ (B = Y, Lu, Sc) at T = 12 K[a]

Perovskite	Peak intensity ratio R_I = ZPL/ν_6	$R_{B^{3+}}-R_{Ta^{5+}}$ (Å)	τ_{av} (ms)
Ba_2YTaO_6	0.11	0.26	1.05
Ba_2LuTaO_6	0.13	0.221	0.96
Ba_2ScTaO_6	0.40	0.105	0.87

[a]$R_{B^{3+}}-R_{Ta^{5+}}$ is the ionic radii difference between the B−Ta cations. τ_{av} is the emission lifetime at T = 12 K.

It should be noted that the octahedral site that is occupied by the Mn^{4+} ion in $BaBTaO_6$ (B = Y, Lu, Sc) is centrosymmetric not only with respect to the nearest neighbor

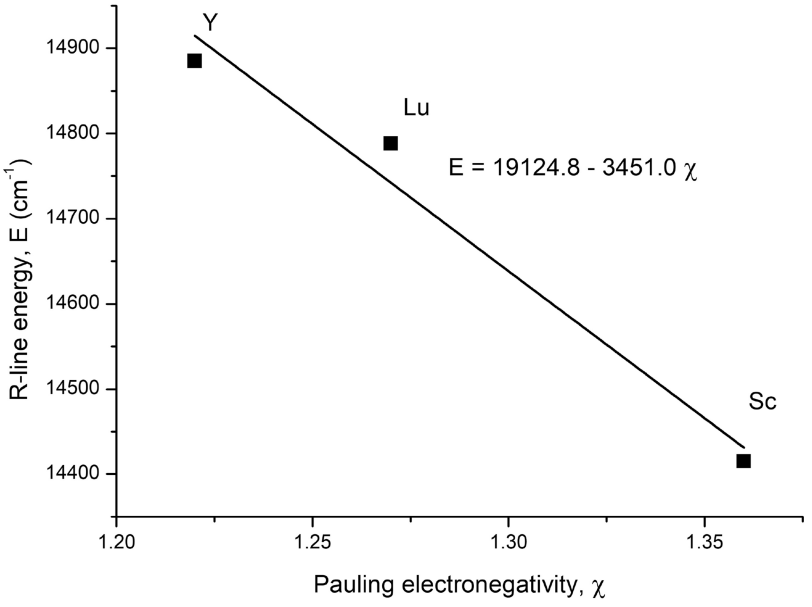

Figure 7. Relationship between the R-line energy and the electronegativity (on the Pauling scale) of the B-cation in Ba_2BTaO_6 (B = Y, Lu, Sc).

https://doi.org/10.1021/acs.jpclett.4c00205
J. Phys. Chem. Lett. 2024, 15, 4175−4184

oxygen ligand coordination but also with respect to the next nearest neighbor cations. In consequence, the R-line is expected to be a magnetic dipole transition with small oscillator strength. The vibronic sidebands which are induced by odd-parity vibrations are electric-dipole allowed and have a much larger oscillator strength. Therefore, R_I in these compounds is expected to be low. The low R_I value in the Y and Lu-phases is in accordance with the expectation. However, R_I is three-times higher in the Sc-phase due to the R-line gaining significant intensity. The interpretation of this result is provided in the following.

For the double perovskite compounds, Barnes et al. have quantified the degree of cation ordering with the long-range order parameter (LRO):[34]

$$LRO = [2 \times (\text{occ.})_M - 1] \times 100 \quad (3)$$

where $(\text{occ.})_M$ is the fractional occupancy of the Ta cation on the octahedral site that is predominantly occupied. For Ba_2ScTaO_6, LRO = 51%.[35] This means that the site occupied preferentially by Ta^{5+} contains 75% Ta^{5+} and 25% Sc^{3+}. For isostructural Ba_2YNbO_6, LRO = 100%.[34] Since the ionic radii of Nb^{5+} and Ta^{5+} are the same in six-coordination, the LRO of Ba_2YTaO_6 = 100%. This implies that the Ta^{5+} site is fully occupied by Ta^{5+} ion.

The cationic mixing model permits the rationalization of results of Table 5. In the double perovskite structure, the Sc−Ta mixing removes the inversion symmetry about the Mn^{4+} ion from the next nearest neighbor cations. The higher R_I value in the Sc-phase is consistent with the R-line gaining oscillator strength due to relaxation of the parity selection rule. The low and similar values of R_I in the Y- and Lu-phases is due to the lack of significant mixing between the Y/Lu−Ta cations. Nonetheless, the ratio is a bit higher in Ba_2LuTaO_6 where the ionic radii difference is smaller (Table 5). Further, the perturbation caused by the cationic mixing accounts for the relatively larger excitation and emission bandwidths in Ba_2ScTaO_6 (Figures 4 and 6). The cationic mixing is a favorable intrinsic defect in the double perovskite structure.

The lifetime of the $Mn^{4+2}E \rightarrow {}^4A_2$ emission transition, which was measured at T = 12 K, is assembled in Table 5. Even at low temperatures, the decay curves deviated from being single exponential. This suggests the presence of multiple Mn^{4+} sites presumably due to the charge compensation mechanism. An average lifetime was calculated using the relationship, $\tau_{av} = \sum_i I_i\tau_i / \sum_i I_i$. The variation of the lifetime with the B-cation is consistent with the expectation of the degree of mixing between the B−Ta cations. The faster radiative lifetime in Ba_2ScTaO_6 is due to the higher oscillator strength of the emission transition due to the considerable Sc−Ta cationic mixing which relaxes the parity section rule. The lifetime in the Lu-phase is faster than that of the Y-phase which is consistent with the smaller difference between the ionic radii of the Lu and Ta cations (Table 5).

In conclusion, the spectroscopic properties of the Mn^{4+} ion have been studied in a series of isostructural double perovskite compounds with the general formula, Ba_2BTaO_6 (B = Y, Lu, Sc). The energy and intensity of the $Mn^{4+2}E \rightarrow {}^4A_2$ emission transition (R-line) are found to depend on the covalence of the $[BTaO_6]$ perovskite framework and on the degree of order between B−Ta cations. The R-line energy decreases as the covalence of the perovskite framework increases, consisting of corner shared BO_6 and TaO_6 octahedrons. This agrees with the expectation of the Tanabe-Sugano diagram for ions with d^3 electronic configuration. The covalence of the perovskite framework is dependent on the electronegativity and the electronic configuration of the B-cation. The intensity of the R-line was found to be dependent on the degree of order between the B−Ta cations. The degree of cationic mixing depends on the ionic radii difference between these cations. Significant mixing occurs in the Sc-phase which lowers the local symmetry about the Mn^{4+} ion. In consequence, the R-line gains considerable intensity in Ba_2ScTaO_6 due to relaxing of the parity selection rule.

It should be noticed that if the coordination octahedron is perfect among the series of compounds (this is a rather rare case), then degree of covalence defining the R-line energy is correlated with the electronegativity of the coordinating cations without other structural interferences (such as decreased hybridization due to octahedral angles deviating from 90°). Based on an in-depth analysis of literature data, this information is the first communication of mentioned above phenomenon in the Mn^{4+}-based red phosphors with double perovskite structures. From the fundamental point of view, our results provide evidence that the spectroscopic data of the Mn^{4+} ion (excitation, emission, and lifetime) can probe and can be an alternative and effective method for investigating the covalence as well as intrinsic disorder of the host lattice. The work also shows that the knowledge gained from the systematic study of the host−Mn^{4+} interaction can serve as a guide to practical improvement and tuning to desired values the key parameters of phosphors.

EXPERIMENTAL SECTION

Since we are interested in correlating the optical properties to the degree of order between B−Ta cations, the samples were prepared under identical conditions. This is because the degree of order between B−Ta cations depends on the synthesis condition. Specifically, the temperature and time of synthesis are of importance.

We followed the procedure of Eng et al. to synthesize the double perovskite compounds.[23] In the first step, the compound (Y, Lu, Sc)$(Ta_{0.99}Mn_{0.01})O_4$ was synthesized by a flux solid-state reaction technique. The starting materials, $(Y, Lu, Sc)_2O_3$, $MnCO_3$, and Ta_2O_5 are mixed with Li_2SO_4 and heated to 1200 °C in air for a period of 10 h.[35] The resulting powder was washed in hot water to remove the Li_2SO_4 flux. The Ba_2BTaO_6:Mn^{4+} (B = Y, Lu, Sc) compounds were synthesized via the following reaction: (Y, Lu, Sc)-$(Ta_{0.99}Mn_{0.01})O_4 + 2BaCO_3 \rightarrow Ba_2(Y, Lu, Sc)(Ta_{0.99}Mn_{0.01})O_6 + 2CO_2$.

The precursor (Y, Lu, Sc)$(Ta_{0.99}Mn_{0.01})O_4$ was mixed with the appropriate amount of $BaCO_3$ and the mixture heated in air to 1300 °C for a period of 10 h in alumina crucible. The resulting powder had a white body color.

The phase purity of the samples was determined by X-ray diffraction (XRD) performed in the range $2\theta = 10°-70°$ with a step $2\theta = 0.02°$ using a Rigaku Miniflex 6 G diffractometer. Cu Kα1 radiation of 1.541 Å wavelength was used. The excitation, emission, and lifetime data were obtained at low temperatures using a closed cycle He system of an Advanced Research Systems cryostat (CS204AE) using Edinburgh FS5 spectrofluorometer.

https://doi.org/10.1021/acs.jpclett.4c00205
J. Phys. Chem. Lett. 2024, 15, 4175−4184

■ ASSOCIATED CONTENT

Supporting Information

The Supporting Information is available free of charge at https://pubs.acs.org/doi/10.1021/acs.jpclett.4c00205.

Transparent Peer Review report available (PDF)

■ AUTHOR INFORMATION

Corresponding Authors

Alok M. Srivastava − *Current Chemicals, Cleveland, Ohio 44110, United States*; Email: srivastaam@outlook.com

Michal Piasecki − *Faculty of Science and Technology, Jan Długosz University, Czestochowa 42200, Poland*; orcid.org/0000-0003-1040-8811; Email: m.piasecki@ujd.edu.pl

Authors

Mikhail G. Brik − *School of Optoelectronic Engineering & CQUPT-BUL Innovation Institute, Chongqing University of Posts and Telecommunications, Chongqing 400065, PR China; Center of Excellence for Photoconversion, Vinča Institute of Nuclear Sciences, National Institute of the Republic of Serbia, University of Belgrade, Belgrade 11351, Serbia; Institute of Physics, University of Tartu, Tartu 50411, Estonia; Academy of Romanian Scientists, Bucharest 050663, Romania*

Chong-Geng Ma − *School of Optoelectronic Engineering & CQUPT-BUL Innovation Institute, Chongqing University of Posts and Telecommunications, Chongqing 400065, PR China*; orcid.org/0000-0001-8090-1738

William W. Beers − *Current Chemicals, Cleveland, Ohio 44110, United States*

William E. Cohen − *Current Chemicals, Cleveland, Ohio 44110, United States*

Complete contact information is available at: https://pubs.acs.org/10.1021/acs.jpclett.4c00205

Notes

The authors declare no competing financial interest.

■ ACKNOWLEDGMENTS

This work was supported by the National Natural Science Foundation of China (Grant Nos. 52161135110 and 12274048), Overseas Talents Plan of Chongqing Association for Science and Technology, China (Grant No. 2022[60]), Polish NCN projects 2021/40/Q/ST5/00336, the Ministry of Science, Technological Development, and Innovation of the Republic of Serbia under contract 451-03-47/2023−01/200017, NCN project 2018/31/B/ST4/00924, and Estonian Research Council grant (PRG 2031).

■ REFERENCES

(1) Cohen, W. E.; Du, F.; Beers, W. W.; Srivastava, A. M. Review—The K_2SiF_6:Mn^{4+} (PFS/KSF) Phosphor. *ECS J. Solid State Sci. Technol.* **2023**, *12*, 076004.

(2) Setlur, A. A.; Radkov, E. V.; Henderson, C. S.; Her, J.-H.; Srivastava, A. M.; Karkada, N.; Kishore, M. S.; Kumar, N. P.; Aesram, D.; Deshpande, A.; Kolodin, B.; Grigorov, L. S.; Happek, U. Energy-Efficient, High-Color-Rendering LED Lamps Using Oxyfluoride and Fluoride Phosphors. *Chem. Mater.* **2010**, *22*, 4076.

(3) Adachi, S. Review - Mn^{4+-}Activated Red and Deep Red-Emitting Phosphors. *ECS J. Solid State Sci. Technol.* **2020**, *9*, 016001.

(4) Rajendran, V.; Chang, Ho; Liu, Ru-Shi; Brik, Mikhail G.; Srivastava, Alok M. Transition metal ion-based phosphors for LED applications. *Luminescent Materials, Fundamentals and Applications* **2023**, *8*, 185 DOI: 10.1515/9783110607871-008.

(5) Srivastava, A. M.; Brik, M. G.; Comanzo, H. A.; Beers, W. W.; Cohen, W. E.; Pocock, T. Spectroscopy of Mn^{4+} in Double Perovskites, La_2LiSbO_6 and La_2MgTiO_6: Deep Red Photon Generators for Agriculture LEDs. *ECS J. Solid State Sci. Technol.* **2018**, *7*, R3158.

(6) Brik, M. G.; Cohen, W.; Payne, S. A.; Cherepy, N. J.; Piasecki, M.; Srivastava, A. M.; et al. On the Mn^{4+} R-line emission intensity and its tunability in solids. *Opt. Mater.* **2019**, *91*, 338.

(7) Brik, M. G.; Srivastava, A. M. On the optical properties of the Mn^{4+} ion in solids. *J. Lumin.* **2013**, *133*, 69.

(8) Brik, M. G.; Srivastava, A. M. Critical Review - A Review of the Electronic Structure and Optical Properties of Ions with d^3 Electron Configuration (V^{2+}, Cr^{3+}, Mn^{4+}, Fe^{5+}) and Main Related Misconceptions. *ECS J. Solid State Sci. Technol.* **2018**, *7*, R3079.

(9) Brik, M. G.; Camardello, S. J.; Srivastava, A. M. Influence of Covalency on the $Mn^{4+2}E_g \rightarrow {}^4A_{2g}$ Emission Energy in Crystals. *ECS J. Solid State Sci. Technol.* **2015**, *4*, R39.

(10) Srivastava, A. M.; Brik, M. G.; Comanzo, H. A.; Beers, W. W.; Cohen, W.; Cherepy, N. J.; Payne, S. A. Optical spectrum of Mn4+ in Y2Ti2-xSnxO7 pyrochlore solid solution: R-line energy and intensity. *Opt. Mater.* **2019**, *95*, 109196.

(11) Jedoń, J.; Lazarowska, A.; Lesniewski, T.; Mahlik, S.; Brik, M. G.; Piasecki, M.; Srivastava, A. M.; Beers, W. W.; Zych, E. Effects of chemically induced cationic disturbance on Mn^{4+} luminescence in double perovskites - temperature and pressure experimental and computational studies. *J. Alloys Compd.* **2023**, *930*, 167435.

(12) Antić, Ž.; Đorđević, V.; Ristić, Z.; Srivastava, A. M.; Brik, M. G.; Dramićanin, M. D.; et al. Influence of composition on the emission properties of impurities in solids: Case study of $Mg_{1-x}Zn_xAl_2O_4$:Cr^{3+} with the spinel structure. *J. Lumin.* **2023**, *264*, 120190.

(13) Srivastava, A. M.; Smith, D.; Brik, M. G. Site occupancy and spectroscopic properties of Mn^{4+} in double perovskites, La_2MgGeO_6. *Opt. Mater.* **2019**, *94*, 148.

(14) Brik, M. G.; Srivastava, A. M.; Beers, W. W.; Cohen, W. E. Optical spectra of Mn^{4+} in double perovskites Ba_2LnNbO_6 (Ln= La, Gd, Y). *Opt. Mater. X* **2021**, *12*, 100089.

(15) Srivastava, A. M.; Gudel, H. U.; Beers, W. W.; Brik, M. G.; Cohen, W. W. Influence of Magnetic Gd^{3+}Ion on the Intensity of Mn^{4+}R-Line in Oxides with Perovskite Structures. *ECS J. Solid State Sci. Technol.* **2021**, *10*, 106002.

(16) Anderson, M. T.; Greenwood, K. G.; Taylor, G. A.; Poeppelmeier, K. R. Effect of the Cation Size Disorder at the A-Site on the Structural Properties of $SrAFeTiO_6$ Double Perovskites (A = La, Pr or Nd). *Prog. Solid St. Chem.* **1993**, *22*, 197.

(17) Momma, K.; Izumi, F. ″VESTA 3 for three-dimensional visualization of crystal, volumetric and morphology data,″. *J. Appl. Crystallogr.* **2011**, *44*, 1272−1276.

(18) Shannon, R. D. Revised Effective Ionic Radii and Systematic Studies of Interatomic Distances in Halides and Chalcogenides Acta Crystallogr. *Sect. A Cryst. Phys. Diffr. Theor. Gen. Crystallogr.* **1976**, *A32*, 751.

(19) Figueiredo, D. S.; Mattos, E. F. d. S.; Araujo, R. M. Computer Modelling of Defects in Ba_2YNbO_6. *J. Phys.: Conf. Ser.* **2022**, *2298*, 012006.

(20) Himanshu, A. K.; Kumar, S.; Dey, U.; Ray, R. Multiple low-energy excitons and optical response of d^0 double perovskite Ba_2ScTaO_6. *Physica B* **2022**, *637*, 413856.

(21) Fang, Y.; Wang, C.; Zhang, Y.; Zhao, G.; Liu, Y.; Liu, Z.; Lin, C. C.; Hou, J. Preparation of far-red emitting Ba_2YTaO_6:Mn^{4+} phosphors for plant growth LEDs applications. *Inorg. Chem. Commun.* **2021**, *128*, 108568.

(22) Kang, X.; Yang, W.; Ling, D.; Jia, C.; Lü, W. A novel far-red emitting phosphor activated Ba_2LuTaO_6:Mn^{4+}: Crystal structure, optical properties and application in plant growth lighting. *Mater. Res. Bull.* **2021**, *140*, 111301.

(23) Eng, H. W.; Barnes, P. W.; Auer, B. M.; Woodward, P. M. Investigations of the electronic structure of d0 transition metal oxides belonging to the perovskite family. *J. Solid St. Chem.* **2003**, *75*, 94.
(24) Halder, S.; Sariful Sheikh, Md.; Ghosh, B.; Sinha, T. P. Electronic structure and electrical conduction by polaron hopping mechanism in A_2LuTaO_6 (A= Ba, Sr, Ca) double perovskite oxides. *Ceramic International* **2017**, *43*, 11108.
(25) Srivastava, A. M.; Brik, M. G.; Comanzo, H. A. Luminescence of Bi^{3+} in the double perovskite, La_2MgTiO_6. *Opt. Mater.* **2018**, *75*, 809.
(26) Srivastava, A. M.; Brik, M. G.; Beers, W. W.; Brik, M. G.; Srivastava, A. M. Luminescence of Bi^{3+} in oxides with perovskite structures. *Luminescent Materials* **2023**, *11*, 271 DOI: 10.1515/9783110607871-011.
(27) Brik, M. G.; Srivastava, A. M.; Ma, C.-G.; Piasecki, M. Dependence of the Mn^{4+} spectroscopic properties on the host composition: Case study of stannate pyrochlores $A_2Sn_2O_7$ (A = La, Gd, Y, Lu). *J. Lumin.* **2020**, *218*, 116834.
(28) Blasse, G.; Bril, A. Photoluminescent Efficiency of Phosphors with Electronic Transitions in Localized Centers. *J. Electrochem. Soc.* **1968**, *115*, 1067.
(29) Tanner, P. A.; Pan, Z. Luminescence Properties of Lanthanide and Transition Metal Ion-Doped Ba_2LaNbO_6: Detection of MnO_6^{8-} and CrO_6^{9-} Clusters. *Inorg. Chem.* **2009**, *48*, 11142.
(30) Srivastava, A. M.; Comanzo, H. A.; Smith, D. J.; Choi, J. W.; Brik, M. G.; Beers, W. W.; Payne, S. A. Spectroscopy of Mn^{4+} in orthorhombic perovskite, $LaInO_3$. *J. Lumin.* **2019**, *206*, 398.
(31) Srivastava, A. M.; Brik, M. G.; Comanzo, H. A.; Beers, W. W.; Cohen, W.; Cherepy, N.; Payne, S. A. Luminescence of Mn^{4+} in the Orthorhombic Perovskites, $ASnO_3$ (A = Ca, Sr). *ECS J. Solid State Sci. Technol.* **2020**, *9*, 016009.
(32) Henderson, B.; Imbush, G. F. *Optical Spectroscopy of Inorganic Solids*; Clarendon Press: Oxford, 1989.
(33) Uylings, P. H. M.; Raassen, A. J. J.; Wyart, J. F. Energies of N equivalent electrons expressed in terms of two-electron energies and independent three-electron parameters: a new complete set of orthogonal operators. II. Application to $3d^N$ configurations. *J. Phys. B: Atom. Mol. Phys.* **1984**, *17*, 4103.
(34) Barnes, P. W.; Lufaso, M. W.; Woodward, P. M. Structure determination of $A_2M^{3+}TaO_6$ and $A_2M^{3+}NbO_6$ ordered perovskites: octahedral tilting and pseudosymmetry. *Acta Crystallogr.* **2006**, *B62*, 384.
(35) Issler, S. L.; Torardi, C. C. Solid state chemistry and luminescence of X-ray phosphors. *J. Alloys Compd.* **1995**, *229*, 54.

https://doi.org/10.1021/acs.jpclett.4c00205
J. Phys. Chem. Lett. 2024, 15, 4175−4184